Higgs Paper Discussion

Mark Thomson
for the editorial team
(Christian, Frank, Mark, Philipp, Strahinja)

Eur. Phys. J. C manuscript No.
(will be inserted by the editor)

Higgs Physics at the CLIC e^+e^- Linear Collider*

First Author[1], Second Author[2,3]

[1]First Address, Street, City, Country
[2]Second Address, Street, City, Country
[3]*Present Address:* Street, City, Country

Overview

- ★ **Getting to where we are today has been a big effort from many people – thank you!**
- ★ **We are approaching the home straight**
  - introductory sections are complete
  - majority of analysis sections exist in some form
  - Now at the point where collaboration-wide input is needed
  - first "pre-draft" (rev180) released to collaboration for initial comments
  - current draft available from nightly build:
    http://proloff.web.cern.ch/proloff/clichiggspaper/

- ★ **Lots of progress, but not there yet…**
  - Summarized in next for pages

Where are we?

- ★ **The released draft – is not yet complete**
- ★ **At this stage requesting comments on specific aspects:**
  - the overall structure of the paper;
  - detailed comments on sections 1 - 3 (which are essentially complete);
  - general comments on sections 4 -10;
  - places where there is too much/too little detail;
  - have we selected the correct figures?

    [Note: plots format/consistency not yet addressed]

Structure

1)	Introduction	[complete]
2)	Overview of Higgs Production at CLIC	[complete]
3)	MC, Detector Simulation and Event Samples	[complete]
4)	Higgs production at 350 GeV	[some gaps + needs polishing]
5)	WW Fusion at > 1 TeV	[some gaps + needs polishing]
6)	ZZ Fusion	[essentially complete]
7)	Top Yukawa Coupling	[essentially complete]
8)	Higgs Self-Coupling	[essentially complete]
9)	Higgs Mass	[missing]
10)	Combined Fit	[needs final numbers]
11)	Summary and Conclusions	[not yet final]

Comments on overall structure ?

Comments on Section 1?

Eur. Phys. J. C manuscript No.
(will be inserted by the editor)

Higgs Physics at the CLIC Electron-Positron Linear Collider*

First Author[1], **Second Author**[2,3]

[1]First Address, Street, City, Country
[2]Second Address, Street, City, Country
[3]*Present Address:* Street, City, Country

Received: date / Accepted: date

Abstract CLIC is an attractive option for a future e^+e^- collider operating at centre-of-mass energies up tp 3 TeV, providing sensitivity to a wide range of new physics phenomena and precision physics measurements at the energy frontier. This paper presents the Higgs physics reach of CLIC operating in three energy stages, $\sqrt{s} = 350$ GeV, 1.4 TeV and 3.0 TeV. The initial stage of operation would allow study of Higgs production from the Higgsstrahlung and WW-fusion process, resulting in a measurement precision of 1.6 % on the $\sigma(e^+e^- \to HZ)$, a measurement of the Higgs total decay width Γ_H with a precision of $\pm x$ MeV, and model-independent measurements of the Higgs couplings to fermions and bosons to between 1 % – 4 %. Operation at $\sqrt{s} > 1$ TeV provides high-statistics samples of Higgs bosons produced through the WW fusion process and gives access to rarer processes such as $e^+e^- \to t\bar{t}H$ and $e^+e^- \to HH\nu_e\bar{\nu}_e$. Studies of these rare processes would provide measurements of the top Yukawa coupling to ±4.5 % and the Higgs boson self-coupling to $\pm y$%. In addition, the high-statistics samples of $e^+e^- \to H\nu_e\bar{\nu}_e$ would provide tight constraints on the Higgs boson couplings, for example, many of the model-dependent κ parameters, adopted by the LHC, would be determined with a precision of between 0.1 % – 1 %. The CLIC programme of precision Higgs measurements would provide a window to physics Beyond the Standard Model (BSM), where for example, Supersymmetric (SUSY) or composite Higgs models can produce significant deviations from the expected SM Higgs branching fractions.

1 Introduction

The Compact Linear Collider (CLIC) is a TeV scale high-luminosity linear e^+e^- collider that is currently under development at CERN. It is based on a novel two-beam acceleration technique providing acceleration gradients of 100 MV/m. Recent implementation studies for CLIC have converged towards a staged approach offering a unique physics program spanning several decades. In this scheme, CLIC would provide high-luminosity e^+e^- collisions from a few hundred GeV to 3 TeV. The nominal centre-of mass energy of the first energy stage is chosen to be $\sqrt{s} = 350$ GeV. For this centre-of-mass energy, the Higgsstrahlung and WW-fusion processes have significant cross sections, giving access to precise measurement of absolute values of Higgs couplings to both fermions and bosons. Another advantage of operating the first stage of CLIC at $\sqrt{s} \sim 350$ GeV is that it enables a programme of precision top-quark physics, including a scan of the $t\bar{t}$ cross section close to the production threshold. In practice, the centre-of-mass energy of the second stage of CLIC operation would be motivated by both the machine design and the results from the LHC. Here it is assumed that the second CLIC energy stage has $\sqrt{s} = 1.4$ TeV and that the ultimate CLIC centre-of-mass energy is 3 TeV. In addition to direct and indirect searches for BSM phenomena, these higher energy stages of operation provide a rich potential for Higgs physics beyond that accessible at lower energies, such as the direct measurement of the top-Yukawa coupling and a direct probe of the Higgs potential through the measurement of the Higgs self-coupling λ. Furthermore, rare Higgs boson decays become accessible due to the higher integrated luminosities at higher energies and the increasing cross section for Higgs production in WW-fusion.

1.1 Experimental Conditions at CLIC

The CLIC accelerator design is based on a two-beam acceleration scheme. It uses a high-intensity drive beam to ef-

*Corresponding Editors: clicdp-higgs-paper-editors@cern.ch

ficiently generate radio frequency (RF) power at 12 GHz. The RF power is used to accelerate the main particle beam that runs in parallel to the drive beam. CLIC uses normal-conducting accelerator structures, operated at room temperature. These structures permit high acceleration gradients, while the short pulse duration discussed below limits ohmic losses to tolerable levels. The initial drive beams and the main electron/positron beams are generated in the central complex and are then injected at the end of the two linac arms. The feasibility of the CLIC accelerator has been demonstrated through prototyping, simulations and large-scale tests, as described in the conceptual design report [1]. In particular, the two-beam acceleration at gradients exceeding 100 MV/m has been demonstrated in the CLIC test facility, CTF3. High luminosities are achieved by very small beam emittances, which are generated in the injector complex and maintained during transport to the interaction point.

CLIC is operated with bunch trains with a repetition rate of 50 Hz. Each bunch train consists of 312 individual bunches, with 0.5 ns between bunch crossings at the interaction point. The average number of high-q^2 interactions in a single bunch train is much less than one. However, for CLIC operation at $\sqrt{s} > 1$ TeV, the highly-focussed intense beams lead to significant beamstrahlung (radiation of photons from electrons/positrons in the electric field of the other beam). Beamstrahlung results in high rates of incoherent electron–positron pairs and low-Q^2 t-channel multi-peripheral $\gamma\gamma \to$ hadron events. In addition, the energy loss through beamstrahlung generates a long lower energy tail to the luminosity spectrum that extends well below the nominal centre-of-mass energy, although this has limited impact on the Higgs physics programme at CLIC. Both the CLIC detector design and the event reconstruction techniques employed are optimized to mitigate the influence of these backgrounds, which are most severe at the higher CLIC energies.

The baseline machine design allows for up to 80 % electron polarisation, but no positron polarisation. Most studies presented in this paper are performed for zero beam polarisation and are subsequently scaled to account for the increased cross sections with left-handed polarisation for the electron beam.

1.2 Detectors at CLIC

The detector concepts used for the CLIC physics studies, described here and elsewhere, are based on the SiD [2, 3] and ILD [3, 4] detector concepts for the International Linear Collider (ILC). They were initially adapted for the CLIC 3 TeV operation, which constitutes the most challenging environment for the detectors. For most sub-detector systems, the 3 TeV detector design is suitable at all energy stages. The only exception being the inner tracking detectors and the vertex detector, where the lower backgrounds at $\sqrt{s} = 350$ GeV enable detectors to be deployed with a smaller inner radius.

The key performance parameters of the CLIC detector concepts with respect to the Higgs program are:

– excellent track momentum resolution, required for a precise reconstruction of leptonic Z decays in HZ events;
– precise impact parameter resolution to provide precise vertex reconstruction, enabling flavour tagging with clean b-, c- and light-quark jet separation;
– jet energy resolution $\sigma_E/E \lesssim 3.5\%$ for jet energies in the range 100 GeV to 1 TeV, required for the reconstruction of hadronic Z decays in HZ events and separation of $W \to q\bar{q}$, $Z \to q\bar{q}$ and $H \to q\bar{q}$ based on the reconstructed di-jet invariant mass;
– detector coverage for electrons extending to far forward angles to maximize background rejection for WW-fusion events.

The main design driver for the CLIC (and ILC) detector concepts is the required jet energy resolution. As a result, the CLIC detector concepts, CLIC_SID and CLIC_ILD, are based on fine-grained electromagnetic and hadronic calorimeters (ECAL and HCAL), optimised for particle-flow analysis (PFA) techniques. In the particle-flow approach, the aim is to reconstruct the individual final-state visible particles within a jet by combining the information from precise tracking with highly granular calorimetry [5, 6]. In addition, particle flow event reconstruction provides a powerful tool for the rejection of beam-induced backgrounds [7]. The CLIC detector concepts employ strong central solenoid magnets, located outside the HCAL, providing an axial magnetic field of 5 T in CLIC_SID and 4 T in CLIC_ILD. The CLIC_SID concept employs central silicon strip tracking detectors, whereas CLIC_ILD assumes a large central gaseous Time Projection Chamber. In both concepts, the central tracking system is augmented with silicon-pixel and silicon-strip based inner tracking detectors. The two detector concepts are shown schematically in Figure 1 and are described in detail in [7].

1.3 Assumed Staged Running Scenario

The studies presented in this paper are based on a concrete staging scenario for CLIC, which assumes a three-stage implementation. The first stage provides a centre-of-mass energy above 350 GeV to reach the top-pair production threshold. The second stage extends up to $\sqrt{s} = 1.4$ TeV. This was chosen because it is the energy that can be reached with a single CLIC drive-beam complex. The third stage reaches $\sqrt{s} = 3$ TeV, the ultimate energy of CLIC. At each stage,

2

Comments on Section 2

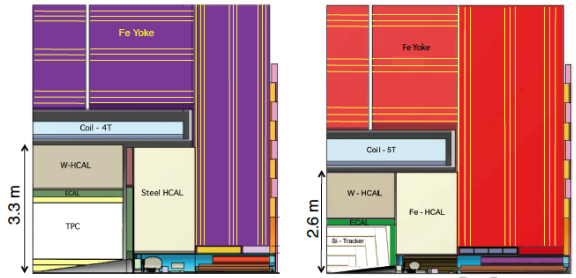

Fig. 1: Longitudinal cross section (to scale) of the top right quadrant of the CLIC_ILD (left) and CLIC_SID (right) detector concepts for CLIC.

four to five years of running with a fully commissioned machine are foreseen, providing integrated luminosities of 500 fb^{-1}, 1.5 ab^{-1} and 2 ab^{-1} at 350 GeV, 1.4 TeV and 3 TeV, respectively.

2 Overview of Higgs Production at CLIC

A high-energy e^+e^- collider, such as CLIC (or the ILC), provides a clean experimental environment to study the properties of the Higgs boson with high precision. The Feynman diagrams for the three highest cross section Higgs production processes at CLIC are shown in Figure 2. In the initial stage of CLIC operation at $\sqrt{s} \approx 350$ GeV, the Higgsstrahlung process ($e^+e^- \to ZH$) has the largest cross section, but the WW-fusion process ($e^+e^- \to H\nu_e\bar{\nu}_e$) is also significant. The combined study of these *two* processes probes the Higgs boson properties (width and branching ratios) in a *model-independent* manner. In the higher energy stages of CLIC operation (1.4 TeV and 3.0 TeV), Higgs production is dominated by the WW-fusion process, with the ZZ-fusion process ($e^+e^- \to He^+e^-$) also becoming significant. Here the relatively large WW-fusion cross section, combined with the high luminosity of CLIC, results in large data samples, allowing precise $\mathcal{O}(1\,\%)$ measurements of the couplings of the Higgs boson to both fermions and the gauge bosons. In addition to the main Higgs production processes, rarer processes such as $e^+e^- \to t\bar{t}H$ and $e^+e^- \to HH\nu_e\bar{\nu}_e$, shown in Figure 3, provide access to the top quark Yukawa coupling and the Higgs trilinear self-coupling as determined by the parameter λ in the Higgs potential. In all cases, the Higgs production cross sections can be increased with polarised electron (and positron) beams.

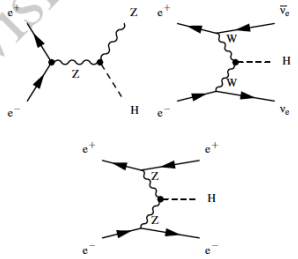

Fig. 2: The three highest cross section Higgs production processes at CLIC.

The evolution of the leading-order e^+e^- Higgs production cross sections with centre-of-mass energy are shown in Figure 4. Table 1 compares the expected numbers of ZH, $H\nu_e\bar{\nu}_e$ and He^+e^- events for the three main CLIC centre-of-mass energy stages. These numbers account the effect of beamstrahlung and initial state radiation (ISR), which result in a tail in the distribution of the effective centre-of-mass energy $\sqrt{s'}$. The impact of beamstrahlung on the expected numbers of events is relatively small. For example, it results in an approximately 10 % reduction in the numbers of $H\nu_e\bar{\nu}_e$ events at $\sqrt{s} > 1$ TeV (compared to the beam spectrum with ISR alone).

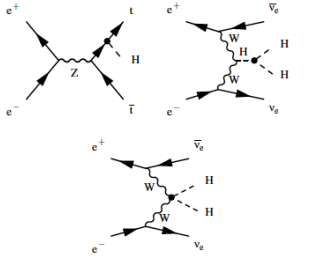

Fig. 3: The main processes at CLIC involving the top-quark Yukawa coupling g_{Htt}, the Higgs boson trilinear self-coupling λ and the quartic coupling g_{HHWW}.

	350 GeV	1.4 TeV	3 TeV
$\mathcal{L}_{int}$	500 fb^{-1}	1500 fb^{-1}	2000 fb^{-1}
$\sigma(e^+e^- \to ZH)$	134 fb	9 fb	2 fb
$\sigma(e^+e^- \to H\nu_e\bar{\nu}_e)$	34 fb	278 fb	479 fb
$\sigma(e^+e^- \to He^+e^-)$	7 fb	28 fb	49 fb
# ZH events	68,000	20,000	11,000
# $H\nu_e\bar{\nu}_e$ events	17,000	370,000	830,000
# He^+e^- events	3,700	37,000	84,000

Table 1: The leading-order Higgs *unpolarised* cross sections for the Higgsstrahlung, WW-fusion, and ZZ-fusion processes for $m_H = 125$ GeV at the three centre-of-mass energies discussed in this document. The quoted cross sections include the effects of ISR but do not include the effects of beamstrahlung. Also listed are the numbers of expected events *including* the effects of the CLIC beamstrahlung spectrum and ISR. The cross sections and expected numbers do not account for the possible enhancements from polarised beams.

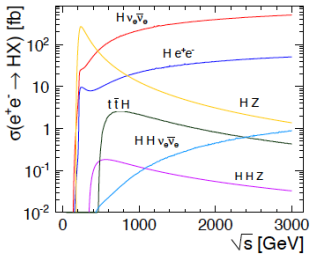

Fig. 4: The centre-of-mass dependencies of the cross sections for the main Higgs production processes at an e^+e^- collider. The values shown correspond to unpolarised beams and do not include the effects of initial-state radiation or beamstrahlung.

The polar angle distributions for single Higgs production at various centre-of-mass energy stages is shown in Figure 5. Most Higgs bosons produced at 350 GeV can be reconstructed in the central parts of the detectors while good capabilties of the detectors in the forward direction are crucial at 1.4 and 3 TeV.

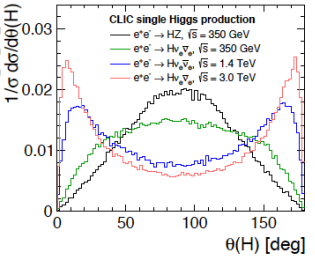

Fig. 5: Polar angle for distributions for single Higgs production at various centre-of-mass energy stages. All distributions include the effects of the CLIC beamstrahlung spactrum and ISR. All distributions are normalised to unity.

A SM Higgs boson with mass of $m_H = 125$ GeV has a wide range of decay modes, as listed in Table 2, providing the possibility to test the SM predictions for the couplings of the Higgs to both gauge bosons and to fermions. All the modes listed in Table 2 are accessible at CLIC.

Decay mode	Branching ratio
$H \to b\bar{b}$	57.7 %
$H \to WW^*$	21.5 %
$H \to gg$	8.6 %
$H \to \tau^+\tau^-$	6.3 %
$H \to c\bar{c}$	2.9 %
$H \to ZZ^*$	2.6 %
$H \to \gamma\gamma$	0.23 %
$H \to Z\gamma$	0.15 %
$H \to \mu^+\mu^-$	0.022 %
Γ_H	4.1 MeV

Table 2: The largest SM Higgs decay modes and branching ratios for $m_H = 125\,\text{GeV}$.

2.1 Motivation for $\sqrt{s} = 350\,\text{GeV}$ CLIC operation

The choice of the CLIC energy stages is motivated by the desire to pursue a programme of precision Higgs physics and to operate the machine above 1 TeV at the earliest possible time; no significant operation is foreseen below the top-pair production threshold. From the perspective of Higgs physics, lower-energy operation is partly motivated by the *direct* and *model-independent* measurement of the coupling of the Higgs boson to the Z, which can be obtained from the recoil mass distribution in $HZ \to He^+e^-$, $HZ \to H\mu^+\mu^-$ and $HZ \to H q\bar{q}$ (see section 4.1.1 and section 4.1.3). These measurements play a central role in the determination of the Higgs couplings at a linear collider. Thus, it might seem surprising that no significant CLIC running is considered at $\sqrt{s} = 250$ GeV, which is close to the maximum of the Higgsstrahlung cross section (see section 4). There are three reasons why 250 GeV operation is not considered a priority. Firstly, the reduction in cross section is, in part, compensated by the increased instantaneous luminosity achievable at a higher centre-of-mass energy; the instantaneous luminosity scales approximately linearly with the centre-of-mass energy, $\mathscr{L} \propto \gamma_e$, where γ_e is the Lorentz factor for the beam electrons/positrons. For this reason the precision on the coupling g_{HZZ} at 350 GeV is comparable to that achievable at 250 GeV for the same period of operation. Secondly, the additional boost of the Z and H at $\sqrt{s} = 350$ GeV provides greater separation between the final-state jets from Z and H decays. Consequently, the measurements of $\sigma(HZ) \times BR(H \to X)$ can be more precise at $\sqrt{s} = 350$ GeV. Thirdly, and most importantly, measurements of the Higgsstrahlung cross section alone are not sufficient to provide truly model-independent measurements of the Higgs boson couplings; knowledge of the total decay width Γ_H is also required. This can be inferred from the measurements of the cross sections for the WW fusion processes. Initial operation of CLIC at $\sqrt{s} \approx 350$ GeV, where the $e^+e^- \to H\nu_e\bar{\nu}_e$ fusion cross section is significant, provides constraints on the Higgs coupling to the W boson and, by inference, provides a determination of Γ_H. For the above reasons, the preferred option for the first stage of CLIC operation is $\sqrt{s} \approx 350$ GeV and operation at $\sqrt{s} \sim 250$ GeV is not foreseen. Furthermore, at $\sqrt{s} \approx 350$ GeV, detailed studies of the top-pair production process can be performed in the initial stage of CLIC operation. Finally, it is worth noting that the Higgs mass can be measured with a similar precision either from the recoil mass distribution in $HZ \to H\mu^+\mu^-$ at $\sqrt{s} = 250$ GeV or from the direct reconstruction of the Higgs decay products in $H \to q\bar{q}$ decays at $\sqrt{s} = 350$ GeV, and again there is no strong argument for operation a the lower energy.

2.2 Impact of Beam Polarisation

The majority of CLIC Higgs physics studies have been performed assuming unpolarised e^+ and e^- beams. However, for the baseline CLIC design, the electron beam can be polarised up to $\pm 80\,\%$ and there is the possibility of positron polarisation at a lower level. For an electron polarisation of P_- and positron polarisation of P_+, the relative fractions of collisions in the different helicity states are

$$e^-_R e^+_R : \tfrac{1}{4}(1+P_-)(1+P_+)\ ,\ e^-_R e^+_L : \tfrac{1}{4}(1+P_-)(1-P_+)$$
$$e^-_L e^+_R : \tfrac{1}{4}(1-P_-)(1+P_+)\ ,\ e^-_L e^+_L : \tfrac{1}{4}(1-P_-)(1-P_+)\,.$$

By selecting different beam polarisations it is possible to enhance/suppress different physical processes. The chiral nature of the weak coupling to fermions results in significant possible enhancements in WW-fusion Higgs production, as indicated in Table 3. The potential gains for the *s*-channel Higgsstrahlung process, $e^+e^- \to ZH$, are less significant, and the $e^+e^- \to He^+e^-$ cross-section dependence on the polarisation is even smaller. In practice, the balance between operation with different beam polarisations will depend on the CLIC physics program taken as a whole, including the searches for and potential measurements of BSM particle production.

2.3 Overview of Higgs Measurements at $\sqrt{s} = 350$ GeV

The Higgsstrahlung process provides the opportunity to study the couplings of the Higgs boson in a *model-independent* manner. This is unique to an electron-positron collider. The clean experimental environment, and the relatively low SM cross sections for background processes, allow $e^+e^- \to ZH$ events to be selected based solely on the measurement of the four-momentum of the Z through its decay products. The clearest topologies occur for $Z \to e^+e^-$ and $Z \to \mu^+\mu^-$ decays, which can be identified by requiring that the di-lepton

Polarisation	Enhancement factor			
$P(e^-) : P(e^+)$	$e^+e^- \to ZH$	$e^+e^- \to H\nu_e\bar{\nu}_e$	$e^+e^- \to Ze^+e^-$	
unpolarised	1.00	1.00	1.00	
$-80\,\% : \ \ 0\,\%$	1.12	1.80	1.12	
$-80\,\% : +30\,\%$	1.40	2.34	1.17	
$-80\,\% : -30\,\%$	0.83	1.26	1.07	
$+80\,\% : \ \ 0\,\%$	0.88	0.20	0.88	
$+80\,\% : +30\,\%$	0.69	0.26	0.92	
$+80\,\% : -30\,\%$	1.08	0.14	0.84	

Table 3: The dependence of the event rates for the *s*-channel $e^+e^- \to ZH$ process and the pure *t*-channel $e^+e^- \to H\nu_e\bar{\nu}_e$ and $e^+e^- \to Ze^+e^-$ processes for three example beam polarisations. The scale factors assume $\sin^2\theta_{eff} = 0.23146$. The numbers are only approximate as they do not account for interference between $e^+e^- \to HZ \to H\nu_e\bar{\nu}_e$ and $e^+e^- \to H\nu_e\bar{\nu}_e$.

invariant mass is consistent with m_Z. The four-momentum of the system recoiling against the Z can be obtained from $E_{rec} = \sqrt{s} - E_Z$ and $\mathbf{p}_{rec} = -\mathbf{p}_Z$. In $e^+e^- \to ZH$ events, the invariant mass of this recoiling system will peak at m_H, allowing the ZH events to be selected based only on the observation of the leptons from the Z decay, providing a model-independent measurement of the Higgs coupling to the Z boson (see section 4.1.1). A slightly less clean, but more precise, measurement can be obtained by repeating the recoil mass analysis for $Z \to q\bar{q}$ decays (see section 4.1.3). The recoil mass studies provides absolute measurement of the total ZH production cross section and provides a model-independent measurement of the coupling of the Higgs to the Z boson, g_{HZZ}. The combination of the leptonic and hadronic decay channels allows g_{HZZ} to be determined with a precision of 0.8 %. In addition, the recoil mass from $Z \to q\bar{q}$ decays provides a direct search for possible Higgs decays to invisible final states, and can be used to constrain the invisible decay width of the Higgs, Γ_{inv}.

By identifying the individual final states for different Higgs decay modes, precise measurements of the Higgs boson branching fractions can be made. Because of the high flavour-tagging efficiencies [7] achievable at CLIC, the $H \to b\bar{b}$ and $H \to c\bar{c}$ decays can be cleanly separated. Neglecting the Higgs decays into light quarks, the branching ratio of $H \to gg$ can also be inferred and $H \to \tau^+\tau^-$ decays can be cleanly identified.

Although the cross section is lower, the *t*-channel WW fusion process $e^+e^- \to H\nu_e\bar{\nu}_e$ is an important part of the CLIC Higgs physics programme at $\sqrt{s} \approx 350$ GeV. Because the final state consists of the Higgs boson decay products alone, the direct reconstruction of the invariant mass of the Higgs boson or, in the case of $H \to WW^*$, its decay products, plays a central role in the event selection. At 350 GeV, the two most important measurements are $\sigma(e^+e^- \to H\nu_e\bar{\nu}_e) \times BR(H \to b\bar{b})$ and $\sigma(e^+e^- \to H\nu_e\bar{\nu}_e) \times BR(H \to WW^*)$, which alongside the other measurements of Higgs production allow the total decay width of the Higgs boson Γ_H to be determined with a precision of $x\,\%$.

2.3.1 Extraction of Higgs Couplings

At the LHC, only *relative* measurements of the couplings of the Higgs boson can be inferred from the data. At an electron-positron linear collider *absolute* measurements of the couplings can be determined using the total $e^+e^- \to ZH$ cross section from the recoil mass analyses. This allows the coupling of the Higgs boson to the Z to be determined with a precision of better than 1 % in an essentially model-independent manner. Once the coupling to the Z is known, the Higgs coupling to the W can be determined from, for example, the ratios of Higgsstrahlung to WW fusion cross sections,

$$\frac{\sigma(e^+e^- \to ZH) \times BR(H \to b\bar{b})}{\sigma(e^+e^- \to \nu_e\bar{\nu}_e H) \times BR(H \to b\bar{b})} \propto \left(\frac{g_{HZZ}}{g_{HWW}}\right)^2 .$$

In order to determine absolute measurements of the other Higgs couplings, the Higgs total decay width needs to be inferred from the data. For a Higgs boson mass of around 125 GeV, the total Higgs decay width in the SM (Γ_H) is less than 5 MeV and cannot be measured directly. However, given that the absolute couplings of the Higgs boson to the Z and W can be obtained as described above, the total decay width of the Higgs boson can be determined from $H \to WW^*$ or $H \to ZZ^*$ decays. For example, the measurement of the Higgs decay to WW^* in the WW-fusion process determines

$$\sigma(H\nu_e\bar{\nu}_e) \times BR(H \to WW^*) \propto \frac{g^4_{HWW}}{\Gamma_H}\,,$$

and thus the total width can be determined utilising the model-independent measurement of g_{HWW}. In practice, a fit (see section 10) is performed to all of the experimental measurements involving the Higgs boson couplings.

2.4 Overview of Higgs Measurements at $\sqrt{s} > 1$ TeV

For CLIC operation above 1 TeV, the large samples of Higgs decays produced in the WW-fusion process allow the relative couplings of the Higgs boson to the W and Z bosons at the $\mathcal{O}(1\,\%)$ level. These measurements provide a strong test of the SM prediction for $g_{HWW}/g_{HZZ} = \cos^2\theta_W$. Furthermore, the exclusive Higgs decay modes can be studied

with significantly higher precision than at $\sqrt{s} = 350$ GeV. For example, CLIC operating at 3 TeV would yield a statistical precision of 1.5 % on the ratio g_{Hcc}/g_{Hbb}, providing a direct comparison of the Standard Model coupling predictions for up-type (charge $+2/3$) and down-type (charge $-1/3$) quarks. In the context of the model-independent measurements of the Higgs branching ratios, the measurement of $\sigma(H\nu_e\bar{\nu}_e) \times BR(H \to WW^*)$ is particularly important. For CLIC operation at $\sqrt{s} \approx 1.4$ TeV, the large number of events allows this cross section to be determined with a precision of 1.4 % (see section 5.3), which when combined with the measurements at $\sqrt{s} \approx 350$ GeV places strong constraints on Γ_H.

Although the WW fusion process has the largest cross section for Higgs production above 1 TeV, other processes are also important. For example, measurements of the ZZ fusion process provides further constraints on the g_{HZZ} coupling. Furthermore, CLIC operation at $\sqrt{s} = 1.4$ TeV and above enables a determination of the top Yukawa coupling from the process $e^+e^- \to t\bar{t}H \to bW^+\bar{b}W^-H$ with a precision of 4.5 % (see section 7). Finally, the self-coupling of the Higgs boson at the HHH vertex is measurable in 1.4 TeV and 3.0 TeV operation. In the SM, the Higgs boson originates from a doublet of complex scalar fields described by the potential

$$V(\phi) = \mu^2\phi^\dagger\phi + \lambda(\phi^\dagger\phi)^2\,.$$

After spontaneous symmetry breaking, this form of the potential gives rise to a trilinear Higgs self-coupling of strength proportional to λv, where v is the vacuum expectation value of the Higgs potential. The measurement of the strength of the Higgs self-coupling therefore provides direct access to the quartic potential coupling λ assumed in the Higgs mechanism. This measurement is an essential part of experimentally establishing the Higgs mechanism as described by the Standard Model. For $m_H = 125$ GeV, the measurement of the Higgs boson self-coupling at the LHC will be extremely challenging even with 3000 fb^{-1} of data (see for example [8]). At a linear collider, the trilinear Higgs coupling can be measured through the $e^+e^- \to ZHH$ and $e^+e^- \to HH\nu_e\bar{\nu}_e$ processes. The achievable precision has been studied for the $e^+e^- \to ZHH$ process at $\sqrt{s} = 500$ GeV in the context of the International Linear Collider (ILC), where the results show that a very large integrated luminosity is required [9]. For this reason, the most favourable channel for the measurement of the Higgs self-coupling is the $e^+e^- \to HH\nu_e\bar{\nu}_e$ process at $\sqrt{s} \geq 1$ TeV. Here the sensitivity increases with increasing centre-of-mass energy and the measurements of the Higgs boson self-coupling (see section 8) form a central part of the CLIC Higgs physics programme; ultimately a precision of approximately 10 % on λ may be achievable.

Section 3

3 Monte Carlo Samples, Detector Simulation and Event Reconstruction

The results presented in the paper are based on detailed Monte Carlo (MC) simulation studies based on: a full set of SM background processes; full GEANT4 [10, 11] based simulations of the CLIC detector concepts; and a full reconstruction of the simulated events.

3.1 Monte Carlo Event Generation

Because of the presence of beamstrahlung photons in the colliding electron and positron beams, it is necessary to generate Monte Carlo (MC) event samples for e^+e^-, $e^+\gamma$, γe^- and $\gamma\gamma$ interactions. The main physics backgrounds, with up to six particles in the final state, were generated using the WHIZARD 1.95 [12] program. In all cases the expected energy spectra for the CLIC beams, including the effects from beamstrahlung and the intrinsic machine energy spread, were used for the initial-state electrons, positrons and beamstrahlung photons. In addition, low-Q^2 processes with quasi-real photons were described using the Weizsäcker-Williams approximation as implemented in WHIZARD. The process of fragmentation and hadronisation was simulated using PYTHIA 6.4 [13] with a parameter set that was tuned to OPAL e^+e^- data recorded at LEP (see [7] for details). The decays of τ leptons were simulated using TAUOLA [14]. The mass of the Higgs boson was taken to be 126 GeV and the decays of the Higgs boson were simulated using PYTHIA with the branching fractions listed in [15]. The events from the different Higgs production channels were simulated separately. To avoid double counting, the Higgs boson mass was set to 12 TeV in the generation of the background samples. Monte Carlo samples for the measurement of the top Yukawa coupling measurement (see section 7) with eight final-state fermions were obtained using the PHYSSIM [16] package; again PYTHIA was used for fragmentation, hadronisation and the Higgs boson decays. A slightly lower value of 125 GeV was assumed for the mass of the Higgs boson in $e^+e^- \to t\bar{t}H$ events.

3.2 Simulation and Reconstruction

The GEANT4 [10, 11] detector simulation toolkits MOKKA [17] and SLIC [18] were used to simulate the detector response to the generated events in the CLIC_ILD and CLIC_SID concepts, respectively. The `QGSP_BERT` physics list was used to model the hadronic interactions of particles in the detectors. The digitisation, namely the translation of the raw simulated energy deposits into detector signals, and the event reconstruction were performed using the MARLIN [19] and `org.lcsim` [20] software packages. Particle flow reconstruction was performed using PandoraPFA [21, 22]. Vertex reconstruction and heavy-flavour tagging is performed using the LCFIplus program [23]. The detailed training of the neutral network classifiers was performed separately for the centre-of-mass energy and the final state of interest.

Because of the 0.5 ns bunch spacing in the CLIC beams, the pile-up of beam-induced backgrounds can impact the event reconstruction and needs to be accounted for. Realistic levels of pile-up from the most important beam-induced background (from the $\gamma\gamma \to$ hadrons process) was included in all the simulated event samples to ensure that the impact on the event reconstruction was correctly modelled. The $\gamma\gamma \to$ hadrons events were simulated separately and a randomly chosen subset corresponding to 60 bunch crossings was superimposed on the physics event before the digitisation step [24]. The impact of the background is small at $\sqrt{s} = 350$ GeV, and is most significant at $\sqrt{s} = 3$ TeV, where approximately 1.2 TeV of energy is deposited in the calorimeters in a time window of 10 ns. A dedicated reconstruction algorithm was developed to identify and remove approximately 90 % of this out-of-time background, using criteria based on the reconstructed p_T of the particle and the mean calorimeter cluster time. A more detailed description can be found in [7].

Jet finding was performed using the FASTJET [25] package. Because of the presence of pile-up from $\gamma\gamma \to$ hadrons, it was found that the `ee_kt` (Durham) algorithm employed at LEP was not optimal for CLIC. Instead the hadron-collider inspired k_t algorithm, with the distance parameter R based on $\Delta\eta$ and $\Delta\phi$, was found to give better performance since it increases distances in the forward region, thus reducing the clustering of the (predominantly low transverse momentum) background particles with those from the hard e^+e^- interaction. The particles clustered into the beam jets are likely to have originated from beam-beam backgrounds, and are removed from the event. As a result of using the R-based k_t algorithm the impact of the pile-up from $\gamma\gamma \to$ hadrons is largely mitigated, even before the timing cuts, described above. Again, details are given in [7]. The choice of R was optimised separately for different analyses. In many of the following studies events are forced into a particular N-jet topology. For example, if an event is forced into a two-jet topology, y_{23} is the k_t value at which the event would be reconstructed as three jets. These "y-cut" variables are widely used in a number of event selections, allowing events to be categorised into different topological final states.

Figures

- **Figures are not the final print-ready versions**
- **But we believe what is shown is OK**
  - Where possible chose physics quantities (e.g. masses, angular distributions) over abstract BDT distributions

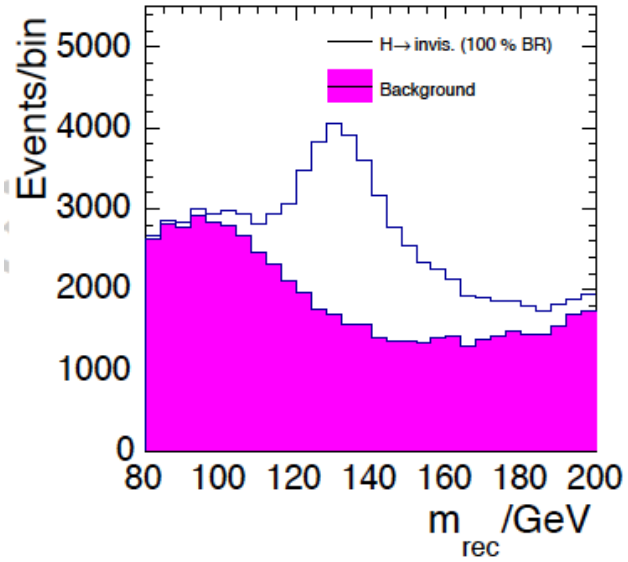

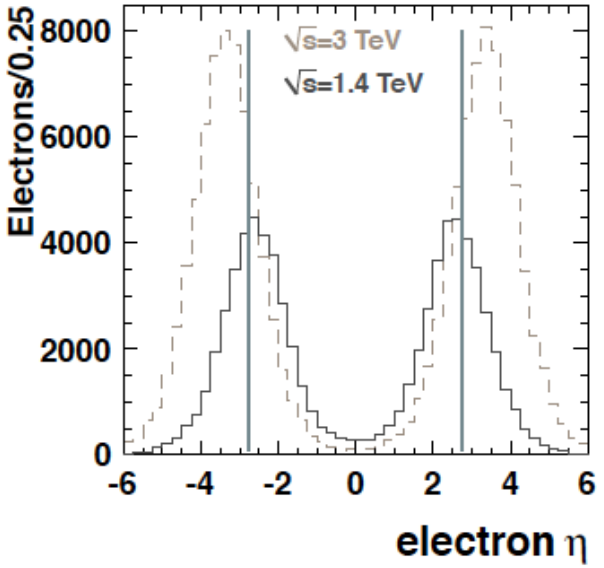

  - Would welcome suggestions on alternative plots

Event displays

e.g. $H \rightarrow \tau\tau$

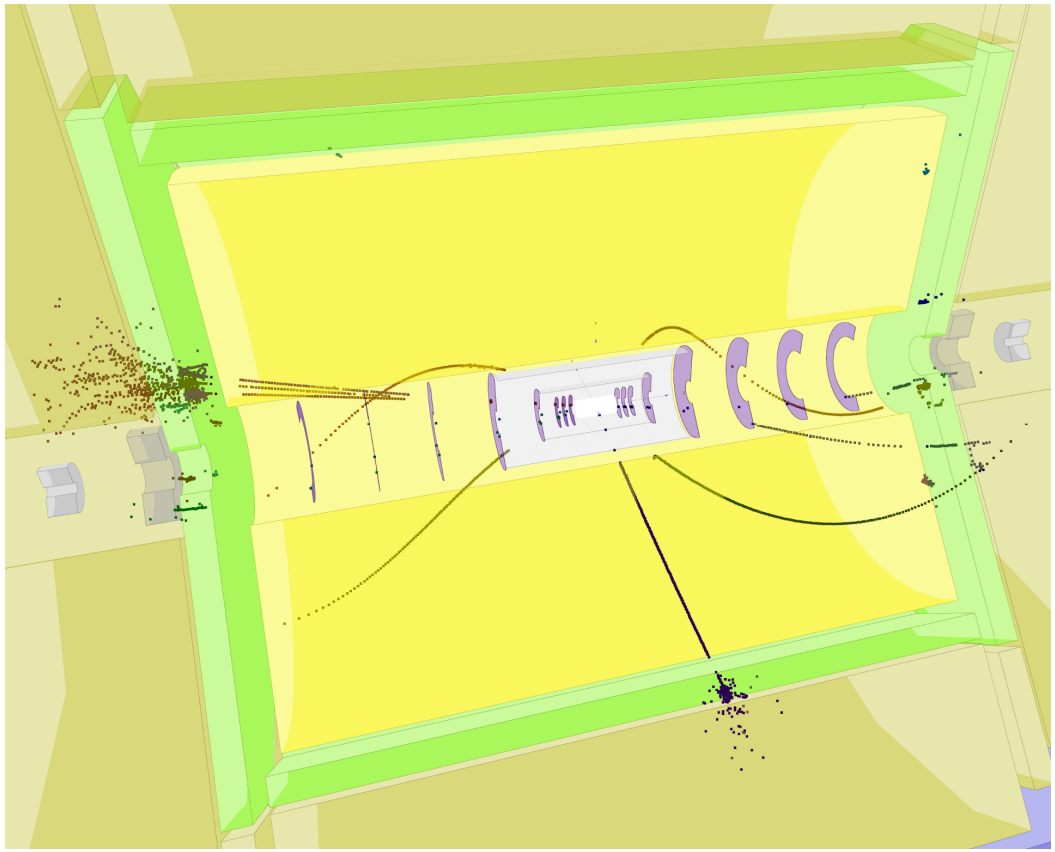

What next?

- **Immediate future:**
  - incorporate comments
  - tie up loose ends with analyses
  - finalize fits (and conclusions)
  - finalize figures

- **As soon as possible:**
  - first full draft released to CLICdp